Primary Voltage Control in Active Distribution Networks via Broadcast Signals: The Case of Distributed Storage

Konstantina Christakou, *Member, IEEE*, Dan-Cristian Tomozei, *Member, IEEE*, Maryam Bahramipanah, Jean-Yves Le Boudec, *Fellow, IEEE*, Mario Paolone, *Senior Member, IEEE*

***Abstract*—In this paper we consider an Active Distribution Network (ADN) that performs primary voltage control using real-time demand response via a broadcast low-rate communication signal. Additionally, the ADN owns distributed electrical energy storage. We show that it is possible to use the same broadcast signal deployed for controlling loads to manage the distributed storage. To this end, we propose an appropriate control law embedded into the distributed electrical storage controllers that reacts to the defined broadcast signal to control both active and reactive power injections. We analyze, in particular, the case where distributed electrical storage systems consist of supercapacitor banks and where the ADN uses the Grid Explicit Congestion Notification (GECN) for real-time demand response developed by the authors in a previous contribution. We estimate the energy reserve required for successfully performing voltage control depending on the characteristics of the network. The performance of the scheme is numerically evaluated on the IEEE 34-node test feeder. We further evaluate the effect of reactive versus active power control depending on the line characteristics. We find that without altering the demand-response signal, a suitably designed controller implemented in the storage devices allows them to successfully contribute to primary voltage control.**

***Index Terms*—Active distribution network, ancillary services, primary voltage control, electrical energy storage systems, broadcast signals, demand response.**

I. Introduction

THE increasing penetration of distributed generation in distribution networks, essentially composed by non-dispatchable resources, renders the control of these networks compelling and calls for active control mechanisms in order to achieve specific operation objectives (e.g., [1], [2], [3], [4], [5], [6], [7]). In particular, grid ancillary services[1] typically employed in the HV transmission networks are expected to be extended to distribution networks, as was recently proposed by the European Network of Transmission System Operators for Electricity (ENTSO-E) [8].

With the increasing availability of communication technologies, we envision that, in distribution networks, these types of ancillary services can be provided by distributed controllable energy resources, such as generators, loads, and energy storage systems. For instance, in [5] the optimal scheduling of generators is proposed for voltage control and minimization of the losses in the network[2]. Furthermore, in [9] electric vehicles are considered for providing frequency-control, whereas in [10] domestic loads are investigated for primary frequency-control. Additionally, forecast uncertainties and increased volatility in the renewable energy production can be tackled by means of local distributed energy storage systems or elastic loads (e.g., [11], [12]).

Most such control schemes rely on two-way communication between the controllable entity and the DNO (e.g. [13], [14]). However, the distributed nature of the controllable resources as well as their large number and small individual impact motivates the use of a control mechanism based on one-way communication. In [15], for instance, the charging rate of electric vehicles is controlled via broadcast signals so as to avoid the overloading of the distribution feeders. Furthermore, the authors in [16] propose the use of a universal broadcast signal to control the charge rate of a fleet of electric vehicles for the local compensation of renewable production volatility.

The present work aims at evaluating whether it is possible to use the same broadcast signal as proposed in [17] to control distributed electrical energy storage systems (ESSs). In the considered scenario, in addition to elastic load control, the DNO can operate the grid via ESSs. ESSs are expected to cover a wide spectrum of applications in distribution networks as they are characterized by charge/discharge cycles that could range from seconds (typically in high-power applications) to hours or even days (in high-energy applications) [18]. As a consequence, ESSs are able to compensate instantaneous imbalances (e.g., fluctuations of renewable generation), to time-shift the energy production or consumption (e.g., slow variations in renewable generation) and, also, to contribute to voltage support (e.g., [19]).

In this paper, we assume that ESSs are employed for primary voltage control and are controlled by the DNO via broadcast signals computed as in [17]. We propose a controller design that properly responds to such signals and that is tailored to the characteristics of the considered storage devices. Within the context of voltage control in active distribution networks (ADNs), it is important to underline that this specific ancillary service requires controlling both active and reactive power injections, in view of the non-negligible R/X ratio

Konstantina Christakou, Dan-Cristian Tomozei, Maryam Bahramipanah, Jean-Yves Le Boudec and Mario Paolone are with the École Polytechnique Fédérale de Lausanne, CH-1015 Lausanne, Switzerland.

[1]By "grid ancillary services" we refer to frequency support, voltage support, black start and island operation capabilities, system coordination and operational measurement. See [8] for further details.

[2]Although the minimization of the losses does not explicitly solve the problem of the lines congestion, it provides a first solution that tends to be in the same direction of the congestion alleviation.

of longitudinal parameters of the medium and low voltage lines (e.g., [20], [21]). To this end, we first discuss the ESSs' rough sizing that is necessary to improve the network voltage profiles. Finally, we investigate the performance of the real-time mechanism when mixed populations of controllable resources with different characteristics (e.g., size, inertia, storage capabilities) are present in the network.

The structure of the paper is the following: in Section II the necessary background on primary voltage control via broadcast signals is presented. Section III focuses on the representation of storage devices and on the description of a specific type of ESS, namely supercapacitors. Also, in the same section, the proposed ESS controller is described together with a way to approximately size these devices. In Section IV the evaluation of the proposed scheme is provided through application examples using the IEEE 34 node test feeder where supercapacitor banks, as well as thermostatically controlled appliances are present in each network bus. Finally, Section V concludes the paper with the final remarks on the benefits and the applicability of the method and with possible future applications.

II. Primary Voltage Control via Broadcast Signals

In this section we give the main background on the principles and operation of the control mechanism proposed in [17], which is called "Grid Explicit Congestion Notification" (GECN). This mechanism acts on a fast time scale and is designed to provide ancillary services to the grid by means of low bit-rate broadcast control signals. In order to provide primary voltage control, GECN relies on the assumption that the DNO controls the consumption of a large population of small dispersed resources in the network in coordination with centralized resources (e.g., on-load tap changers).

The implementation of the scheme is based on the closed-loop control depicted in Fig. 1. First, at every time step, the DNO computes the optimal required power adjustments $\{\mathbf{\Delta}(\mathbf{P})^*(t)\}$ in the buses and, at the same time, the optimal tap-changers positions $\{\mathbf{\Delta n}^*(t)\}$ which lead to the desired operation set-point for voltage control. The DNO can decide whether to simply utilize the distributed resources or a co-ordinated action of the elastic demand and the on-load tap-changers (OLTC). The optimal required power adjustments in the buses and the OLTC positions are computed by penalizing deviations of power injections from available forecasts and voltage deviations from the network rated value via the constrained optimization problem presented in [17]. Then, these set points are mapped to a signal $g(t)$ in the range $[-1, 1]$, where a negative g_i encourages consumption, a positive g_i inhibits consumption, and $g_i = 0$ does not impact the behavior of the controllable resources[3]. Finally, the resulting variation of the aggregate power at the buses provides the DNO with an implicit feedback to the control signal, which is used to estimate the responsiveness of the bus resources and to decide

[3]When the distributed resources can be controlled in terms of active as well as reactive power the same procedure can be adopted to compute signals for both powers set points.

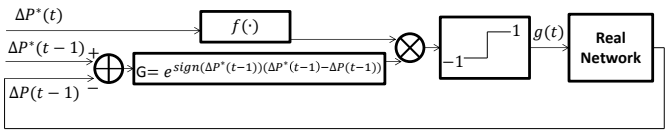

Figure 1. Control loop for GECN signal $\mathbf{g}(t)$. Adapted from [17].

the subsequent control. As it can be inferred from Fig. 1, the broadcast signal at time t is computed as a function of (i) the optimal set points at the current time step and (ii) the mismatch G between the optimal and the actual set points that the DNO observed at the previous time step $t-1$. In [17] the potential of GECN for providing primary voltage control was investigated for the case of thermostatically controlled appliances used to provide the considered ancillary service.

In this work, we are interested in controlling distributed electrical storage; in order to keep the system tractable, we would like to avoid individual point-to-point communication from the DNO's controller to every storage system. It is thus natural to use a broadcast signal, and to rely on state estimation for the feedback channel, as with GECN. We go one step further and ask whether the *same* GECN signal can be used for controlling the ESSs as well. We show that this is indeed possible, without any change to GECN, by defining an appropriate control law implemented in the ESS controllers. In other words, we propose that the same GECN signals are broadcasted to the different buses of the network; it is the local controller of each elastic appliance or storage system that decides the system's response to the received signal.

In the following section, we briefly present the model of a given storage device used in the rest of the paper as well as the design of a controller suitable for their contribution to primary voltage control[4].

III. Electrochemical energy storage representation and control

In this section, the general representation of electrochemical energy storage systems, considered in this paper, is presented and a controller, tailored to the characteristics of storage devices, is proposed.

A. General Formulation of the State-of-Charge of Electrochemical-based Storage Systems

The estimation of the so-called State of Charge (SoC) of an electrochemical-based storage system is of great importance in the majority of applications dealing with operation and control of electrochemical ESSs [22].

Several methods have been proposed in the literature that use different criteria in order to estimate the SoC. As discussed in [23] the five most important criteria, with particular reference to batteries, are (i) measurement of electrolyte specific gravity; (ii) battery current time-integration; (iii) battery impedance/resistance estimation; (iv) measurement of the battery open circuit voltage; and (v) inclusion of electrolyte

[4]The model and the local controller design for thermostatically controlled appliances are described in detail in [17].

temperature, discharge, rate and other battery parameters. A general equation that defines the SoC at a specific time instant and is a combination of the above criteria is (e.g., [22], [24], [25], [26]):

$$SoC(t) = \frac{C(t_0) - \alpha(I,\theta)\int i(t)dt}{C(I,\theta)} \quad (1)$$

where $C(I,\theta)$ is the ESS capacity for a constant current discharge rate I at electrolyte temperature θ, $C(t_0)$ is the ESS capacity at time t_0, $i(t)$ is the instantaneous value of the current and α is the charge-efficiency coefficient associated to charge and discharge phases[5].

In this work, the SoC, computed as in (1), will be incorporated by the storage controller as better discussed in Sec. III-C.

B. Circuit-based Model of Electrochemical ESS Applied to the Case of Supercapacitors

A general approach in modeling electrochemical ESSs is to represent a single cell with an equivalent circuit-based model that simulates their behavior (e.g., [27], [28], [29]). Such models are providing simple structures that can represent sufficiently the dynamic behavior of these ESSs as they are directly related to the physics/chemistry of the cell configuration. The major advantage of this approach is that the relationship between the cell voltage and the current drawn or supplied to the cell can often be analytically expressed by solving a system of ordinary differential equations [30].

In this paper, supercapacitors (SC) have been selected as the targeted energy storage system. Due to their high power density, short charge time and long life duration, these devices are particularly interesting in ESS applications that require fast cycles (e.g., primary voltage control via fast compensation of renewable DG, fast charging of electric vehicles) [31]. Several circuit-based models, that can represent the SC behavior in both steady-state and dynamic conditions, have been proposed in the literature (e.g., [32], [33]). In this work, the model developed in [33] is considered, for which the equivalent circuit model is depicted in Fig. 2. This model allows the correct representation of both the quasi-static and dynamic behavior of a SC accounting, also, for the so-called "redistribution-effect" that plays a major role in its dynamic behavior.

For this specific model the SC terminal voltage, V_{DC}, is linked to the input current, I_{DC}, via the following system of ordinary differential equations:

$$\begin{aligned}
\frac{dV_1}{dt} &= (-(I_{DC}+I_{ch}) + \frac{V_1 - V_2}{R_2} + V_1\frac{dC_v}{dt} - I_{red})\frac{-1}{C_v} \\
\frac{dV_2}{dt} &= (\frac{V_2 - V_3}{R_3} - \frac{V_1 - V_2}{R_2} + V_2\frac{dC_2}{dt})\frac{-1}{C_2} \\
\frac{dV_3}{dt} &= (-\frac{V_2 - V_3}{R_3} + V_3\frac{dC_3}{dt})\frac{-1}{C_3} \\
V_{DC} &= V_1 + (I_{DC}+I_{ch})(R_1+R_L)
\end{aligned} \quad (2)$$

where R_1 is the input electrode resistance; R_L and C_V are the resistance and the capacitance of the so-called "SC network system model"; R_2, C_2 and R_3, C_3 are the resistances and the capacitances of the second and third branch respectively. All the capacitances exhibit a non-linear dependence on the voltage. This dependence is taken into account by curve-fitting measurements obtained via experimental tests. As proposed in [33], the two current sources, I_{ch} and I_{red}, allow for improving the dynamics of the SC by taking into account the diffusion of the residual charge during the charge/discharge phases (short-time phenomenon), as well as during the redistribution phase (long-time phenomenon).

[5]As a first approximation $\alpha(I,\theta)$ can be assumed equal to 1. Specific tests on the targeted storage systems can infer this function.

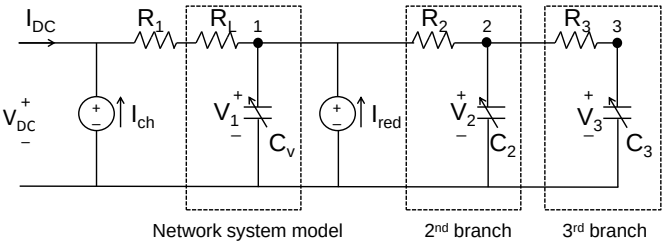

Figure 2. Proposed SC model in [33].

In the rest of the paper we assume that SC cells are arranged in suitable parallel and series connections to form an array of a given total energy and power capacities. A bidirectional DC/AC converter is used to interface the SC with the network. The state of each cell is assumed to be its terminal voltage and the evolution of this state is described by (2). In order to model the power converter, the constraints on the AC active and reactive power should be taken into account. The PQ capability curve of the converter is described by the following inequality constraint:

$$\sqrt{P_{AC}^2 + Q_{AC}^2} \leq S_r \quad (3)$$

where, S_r is the rated power of the converter and P_{AC},Q_{AC} the active/reactive power flows on the AC-side of the power converter interfacing the SC towards the grid.

It is assumed, as a first approximation, that the DC/AC converter is characterized by an efficiency (η) independent of its power flow. It is also assumed that this power converter can operate in four quadrants.

C. Storage Controller

In comparison with [17], where active power signals were used, the storage devices connected to a network bus i receive at each time step t two broadcast control signals, $g_{P_i}(t)$ for the active power and $g_{Q_i}(t)$ for the reactive power. Each signal represents a real number $g_{P_i}(t), g_{Q_i}(t) \in [-1,1]$ coded, for example, on 16 bits. The control signals $g_{P_i}(t), g_{Q_i}(t)$ are proportional to the DNO's desire to inhibit consumption. Hence, a negative g_{P_i} encourages charging, a positive g_{P_i} encourages discharging, and $g_{P_i} = 0$ does not have an effect on the storage devices. Similarly, a negative g_{Q_i} calls for reactive power absorption, a positive g_{Q_i} requests for more reactive power support, and $g_{Q_i} = 0$ means that the DNO is satisfied with the current state of the ESS.

In what follows, we propose a controller that takes into account these signals. As described next, in response to non-zero $g_{P_i}(t), g_{Q_i}(t)$ signals, the SC decides to charge or

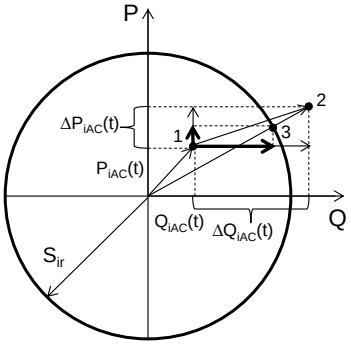

Figure 3. Adjustment of the requested power set points in case of violation of the constraints of the PQ capability curve of the converter.

discharge an amount of energy. This decision is a function of the signals, the SoC, the DC voltage, as well as the previous state of the device. When this decision is made, the controller chooses the next state of the device as follows:
1. Upon receiving $g_{Pi}(t)$ and $g_{Q_i}(t)$, the controller considers the signals as requested adjustments in its AC-side active and reactive power set points:

$$\begin{aligned}\Delta P_{iAC}(t) &= -S_{ir} g_{Pi}(t) \\ \Delta Q_{iAC}(t) &= -S_{ir} g_{Q_i}(t)\end{aligned} \tag{4}$$

In other words, the two signals are viewed as proportional to the desired response of the resources requested by the DNO.
2. The actual response of the device depends on the current operating point $(P_{iAC}(t), Q_{iAC}(t))$, on the SC internal state $(V_{iDC}(t))$ and on its state of charge $(SoC_i(t))$. First, the controller verifies that the constraints on the PQ capability curve of the converter are respected. If this is not the case, $\Delta P_{iAC}(t)$ and $\Delta Q_{iAC}(t)$ are adjusted in such a way that the total power set point is the closest to the circle represented by (3). Fig. 3 shows an example where the requested set points lead the system to a state where the constraints of the converter are violated (point 2 in Fig. 3) and adjustment is required to a new state (point 3 in Fig. 3). Then, the new AC set points are computed as a moving average of the previous operating point and the requested operating set-point filtered by a function of the SoC:

$$\begin{aligned}P_{iAC}(t+1) &= \omega[\beta(P_{iAC}(t) + \Delta P_{iAC}(t))] + (1-\omega)P_{iAC}(t) \\ Q_{iAC}(t+1) &= \omega[\beta(Q_{iAC}(t) + \Delta Q_{iAC}(t))] + (1-\omega)Q_{iAC}(t)\end{aligned} \tag{5}$$

where ω is a fixed gain and β is a function of the current SoC of the SC. Specifically, for the active power $\beta = (1 - SoC_i)^2$, when the device is charging $(P_{iAC}(t) > 0)$, whereas $\beta = (SoC_i)^2$ when the device is discharging $(P_{iAC}(t) < 0)$. For the reactive power, $\beta = (SoC_i)^2$ regardless of the sign of the requested reactive power flow[6]. This coefficient is used to filter the total power provided by the storage devices in order to smooth their response by accounting for their internal state.
3. The internal state constraints of the storage device are finally taken into account. In particular, if the DC voltage has reached a specific minimum (V_{DCmin}) or maximum (V_{DCmax}) value, then the controller refuses to participate in the action to avoid the intervention of the maximum/minimum voltage relays always used in these types of systems to preserve the power electronics [23]. If the limits are not yet reached, the AC set points are transformed in DC power requirements and subsequently, in charging/discharging current references as follows:

$$\begin{aligned}P_{iloss}(t+1) &= (1-\eta_i)\sqrt{P_{iAC}^2(t+1) + Q_{iAC}^2(t+1)} \\ P_{iDC}(t+1) &= P_{iAC}(t+1) + P_{iloss}(t+1) \\ I_{iDC}(t+1) &= \frac{P_{iDC}(t+1)}{V_{iDC}(t)}\end{aligned} \tag{6}$$

where $P_{i_{loss}}$ represents the losses in the i-th power converter. At this point the $V_{i_{DC}}$ is continuously changing as a function of the charging/discharging current $I_{i_{DC}}$ based on the model of the i-th ESS. For instance, in the case of supercapacitors, $V_{i_{DC}}$ is updated based on (2). Then the current is updated so as to maintain the $P_{i_{DC}}$ set point constant, until the controller receives the next GECN signals.

D. On the Sizing of the ESSs

As known, the sizing of an ESS is intimately coupled with its control algorithm. In this respect, this subsection illustrates a possible procedure to size the distributed storage systems to fit the requests of the proposed control algorithm.

The DNO is assumed to have imperfect 24hr forecasts for load and renewable profiles $(\mathbf{P}, \mathbf{Q})_f$ as well as the real measurements corresponding to these profiles. Therefore, the DNO can obtain the expected daily voltage profiles in the network by solving the load flow problem. Once the phasors of the phase-to-ground voltage $\bar{E}_i$ are known, the DNO can compute the voltage sensitivity coefficients with respect to absorbed/injected power of a network bus ℓ [17]:

$$K_{P,i\ell} := \frac{\partial |\bar{E}_i|}{\partial P_\ell},\ K_{Q,i\ell} := \frac{\partial |\bar{E}_i|}{\partial Q_\ell} \tag{7}$$

for instance, by solving the linear systems of equations presented in [21], [34]. Therefore, the following linear relation between variation in bus voltages and variations of active/reactive power set points of the storage systems $\Delta P_i, \Delta Q_i$ can be derived (e.g. [5]):

$$\begin{aligned}\Delta |\overline{E}|_i &\approx \mathbf{K_P}_i \mathbf{\Delta P} + \mathbf{K_Q}_i \mathbf{\Delta Q} \\ &\triangleq (\mathbf{K_{P,Q}}(t) \mathbf{\Delta}(\mathbf{P}, \mathbf{Q}))_i.\end{aligned} \tag{8}$$

Using the sensitivity coefficients $\mathbf{K_{P,Q}}$ the DNO can compute the optimal required power adjustments $\{\mathbf{\Delta}(\mathbf{P}, \mathbf{Q})^*\}$ in the buses which lead to the desired operation set-point for voltage control, for the whole 24hr period, by solving offline the constrained optimization problem:

$$\begin{aligned}&\min_{\mathbf{\Delta}(\mathbf{P},\mathbf{Q})} \sum_i \mu_i \left(\mathbf{\Delta}(\mathbf{P}, \mathbf{Q})_i - \mathbf{\Delta}(\mathbf{P}, \mathbf{Q})_{f_i} \right)^2 + \\ &\sum_i \lambda_i [\left(|\overline{E}_i| + (\mathbf{K_{P,Q,n}}(t) \mathbf{\Delta}(\mathbf{P}, \mathbf{Q}, \mathbf{n}))_i - |\overline{E}| \right)^2 - \delta^2]^+ \\ &\text{subject to:} \quad \gamma_i \leq \cos \varphi_i \leq 1\end{aligned} \tag{9}$$

[6]Note that the request of the reactive power is always draining energy from the SC through the losses in the converter regardless of the sign of the reactive power flow.

where γ_i is the constraint on the power factor, $\cos\varphi_i$, of a specific bus i and the parameter δ denotes the value of the voltage deviation from the network-rated value tolerated by the network operator.

The solution of (9) provides profiles of PQ setpoints for a given scenario of loads and distributed generation. Once the required power adjustments are computed for each bus, the DNO has a rough knowledge of the instantaneous amount of excess or deficit in the active and reactive power throughout the whole 24hr period. Thus, the DNO can compute the energy and, consequently, the size of storage devices that will be needed. In fact, the integral of the active power flow for a given storage system, quantifies the size of this storage system. However, the outcome of such a sizing is related to the considered scenarios.

In our case, the targeted ESSs are SCs. Therefore, since they are characterized by high power density and low energy density, we have taken into account the nature of these devices and we do not aim to utilize them for performing energy balance. To this end, we have assumed as worst-case condition the one that involves large instantaneous errors in the forecasted PV power production. In particular, Fig. 4 shows the actual and forecasted daily profiles of active and reactive power of the whole network used for the sizing of these devices, as well as the forecasting errors.

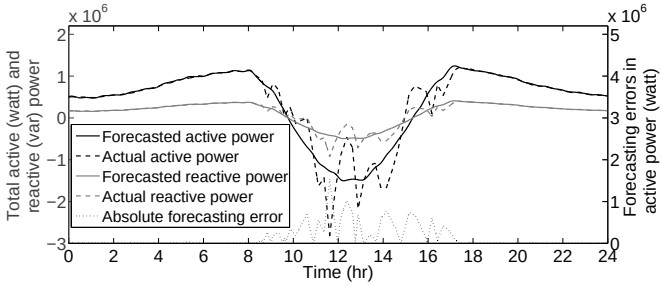

Figure 4. Actual/forecasted values of active and reactive power used for the sizing of the SC arrays.

IV. Evaluation

For the evaluation of the proposed mechanism we have considered the IEEE 34 node test feeder as depicted in Fig. 5. The network load flow problem, the SC model (2), as well as the storage control mechanism are simulated in Matlab.

A. Test cases

It is assumed that each network bus comprises a SC bank, a large population of heterogeneous household controllable loads along with non-elastic demand, as well as non-dispatchable power injections. Concerning the non-dispatchable power generation, we assumed to have a PV-type profile with peak power that changes for all buses within the range of $90\% - 180\%$ of each secondary substation peak load. As far as the forecasting errors are concerned, two different scenarios are considered. In the first scenario we assume to have a good 24hr-ahead forecast whereas in the second scenario we assume to have large forecasting errors.

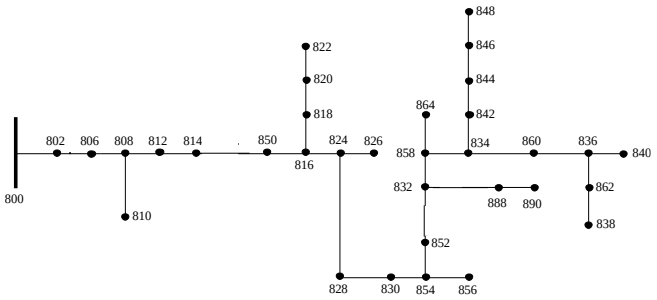

Figure 5. IEEE 34 node test feeder used for the evaluation of the proposed control mechanism [35].

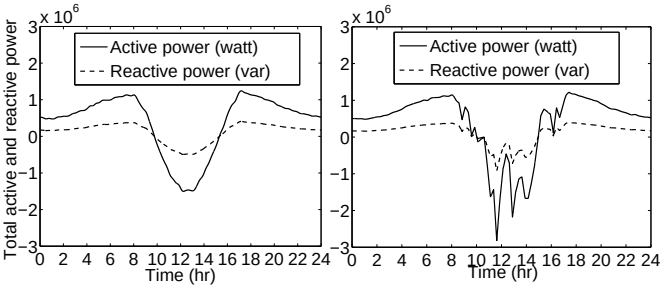

Figure 6. Aggregate network active and reactive power profiles for two different scenarios of forecasting errors in the day-ahead PV production.

Fig. 6 shows the aggregate load profile of all 34 buses in the network for both test cases, where the convention is used that negative values represent power injection and positive power consumption.

B. Storage system sizing

The SC arrays are sized approximately using the procedure described in Sec. III-D. To this end, in (9) γ_i is set to 0.9 for all network buses and δ to 0.04 (see [17] for further details). The number of cells in parallel connection, N_p, for each bus of the network are given in Table I. The number of cells in series, N_s, are equal to 149 for all buses[7]. In the same table, we provide also the available energy of each array, as well as the rated power that is limiting the capabilities of the converter (3). It is worth observing that the amount of energy per bus required by ESS to perform primary voltage control is in the order of few tens of KWh. Such a limited reservoir appears compatible with a specific economic analysis of the use of SC which is beyond the scope of this paper. Additionally, the parameters of the storage controller, used hereafter, are given in Table II.

C. Primary Voltage Control via Distributed Supercapacitors

In this subsection, we evaluate the performance of the designed SC controller. To this end, the DNO employs the broadcast signals, g_{P_i} and g_{Q_i}, described in Sec. III-C.

In order to infer the benefits of using distributed storage for primary voltage control, Fig. 7 shows the initial voltage

[7]The number of cells in series is determined by dividing the maximum voltage required, assumed here 400 Volts, by the SC nominal cell voltage (i.e., $2.7V$).

Table I
NUMBER, CAPACITY AND RATED POWER OF ESS PER NETWORK BUS

Bus N_o	N_p	Energy(kWh)/ Power(MW)	Bus N_o	N_p	Energy(kWh)/ Power(MW)
800	-	-	856	49	26.61 / 0.876
802	28	15.21 / 0.501	852	64	34.76 / 1.144
806	56	30.41 / 1.001	832	74	40.19 / 1.323
808	30	16.29 / 0.536	888	43	23.35 / 0.769
810	65	35.30 / 1.162	890	50	27.16 / 0.894
812	43	23.35 / 0.769	858	57	30.96 / 1.019
814	58	31.50 / 1.037	864	75	40.73 / 1.341
850	65	35.30 / 1.162	834	46	24.98 / 0.823
816	34	18.47 / 0.608	842	51	27.70 / 0.912
818	44	23.90 / 0.787	844	65	35.30 / 1.162
820	50	27.16 / 0.894	846	50	27.16 / 0.894
822	65	35.30 / 1.162	848	85	46.16 / 1.520
824	39	21.18 / 0.697	860	54	29.33 / 0.966
826	42	22.81 / 0.751	836	66	35.84 / 1.180
828	58	31.50 / 1.037	862	76	41.28 / 1.359
830	43	23.35 / 0.769	838	45	24.44 / 0.805
854	78	42.36 / 1.395	840	52	28.24 / 0.930

Table II
PARAMETERS OF THE STORAGE CONTROLLER

Parameter	value
Voltage deadband of single cell, V_{DC} (Volts)	[0.8,2.7]
Capacity of single cell, C_{cell} (F)	3600
Gain, ω	0.2
Converter efficiency, η	0.95

profile in the network as well as the improvement due to the SC response for both test cases presented in Sec. IV-A. For the sake of brevity, we show the median value of the network voltages at every time step (solid line) along with the relevant 99% confidence intervals (dashed lines). In scenario 1 the improvement in the voltage profile is in the order of 2%. The largest advantage of the proposed control mechanism emerges in the case of large forecasting error where the maximum improvement in the daily voltage profile is in the order of 6%. In Fig. 8 the median value of the SoC of the SC arrays is shown, as well as the relevant 99% confidence intervals.

Finally, we show in Fig. 9, the GECN signals for the active and reactive power for a single network bus. One can observe that when the forecasting errors are small the request for reactive power is larger than the one for active power. As explained later this is due to the ratio of R/X of the network lines. On the contrary, under large errors in the day-ahead PV production, the GECN signal adapts itself and becomes significantly larger for the active than for the reactive power.

D. On the Adequacy of volt/var Control in ADNs

Traditionally, voltage control is related to reactive power control (e.g. static var compensators) [36]. This is true in the case of HV transmission networks or, in general, networks where the ratio of the longitudinal line resistance versus reactance is small and the decoupling of the active and reactive power is a valid approximation. However, such an assumption is no longer applicable to distribution networks that require in addition to take into account active power injections when performing voltage control.

In what follows, we investigate the importance of active versus reactive power support for voltage control in these

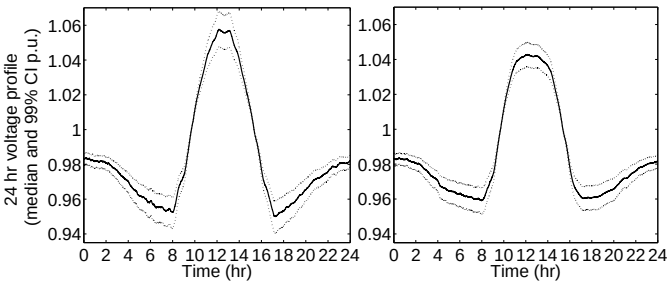

(a) Base case and improved voltage profiles for Scenario 1

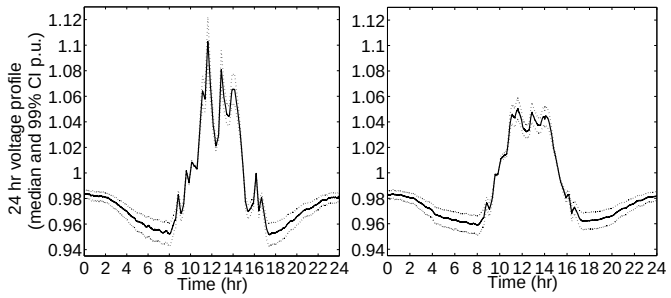

(b) Base case and improved voltage profiles for Scenario 2

Figure 7. Base case and improved 24hr network voltage profiles for two different scenarios of forecasting errors in the PV production.

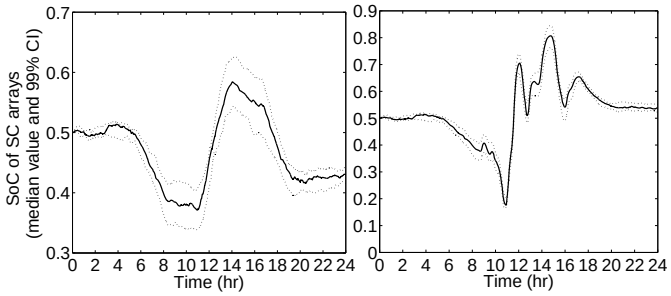

Figure 8. 24hr SoC of the SC arrays for two different scenarios of forecasting errors in the PV production.

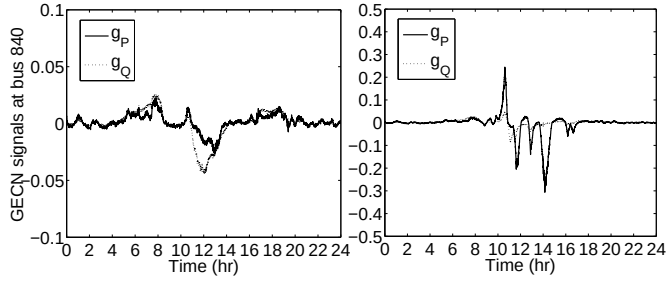

Figure 9. 24hr GECN signals sent to bus 840 for two different scenarios of forecasting errors in the PV production.

specific networks. To this end we vary the resistance of the lines and we observe the optimal ΔP^* and ΔQ^* that are able to improve the voltage profile. Fig. 10 depicts the optimal active and reactive power adjustments for different values of the ratio R/X of the lines. Specifically, the line resistances are varied from 0.25 to 2.75 times their initial value while the line inductances are kept constant. The figure shows the values of the optimal active and reactive power adjustments ΔP^* and ΔQ^* of bus 840 at a specific time-instant. These values are

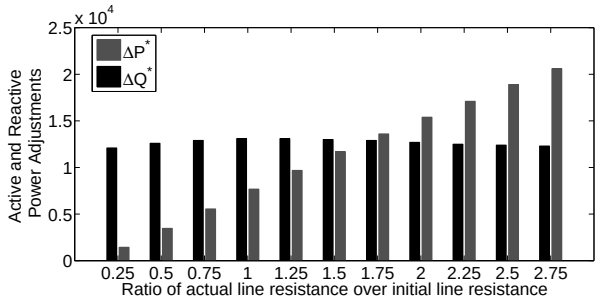

Figure 10. Optimal active and reactive power adjustments necessary to improve the voltage by 2% as a function of the line parameters.

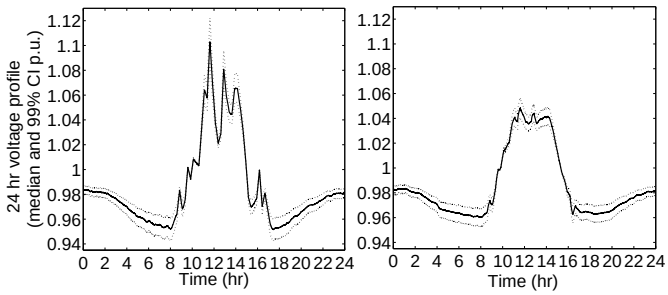

Figure 11. Base case and improved 24hr network voltage profiles when both SC and TCL respond to GECN.

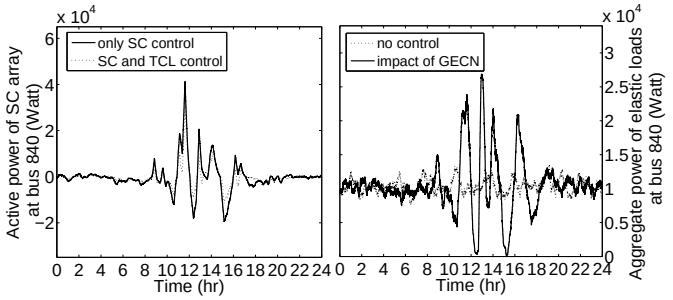

Figure 12. Active power of the SC array and the elastic appliances when only supercapacitors are controlled and when both populations respond to the GECN signals.

computed in order to improve the network voltage profile by 2%. One can observe that as the value of the line resistance is increasing, i.e., when the ratio R/X of the lines is increasing, the optimal active power adjustments are linearly dependent to the R/X ratio, and are becoming more important than the relevant reactive power adjustments.

This observation has two implications. First, as in distribution networks the ratio R/X of the lines is, in general, not negligible, the active power support is necessary when performing primary voltage control. Thus, engaging demand response and ESS control mechanisms in the context of primary voltage control is important. Second, the network characteristics are directly impacting the sizing of the storage devices.

E. Coordination of Heterogeneous Populations for Primary Voltage Control

This subsection shows that heterogeneous controllable resources in the network can contribute to primary voltage control, by responding to the same GECN signal. We consider only scenario 2 and in addition to the SC arrays, in each network bus, a large population of elastic thermostatically controlled loads (TCLs) (e.g., [17]). Specifically, the elastic loads represent 20% of the demand in each network bus. We assume that the local controllers of the elastic appliances, as well as the broadcast signals sent to the controllable resources, are as described in [17]. The DNO coordinates with the same signal the loads and the SCs.

In order to quantify the improvement in the network voltage profile due to the coordinated response of the different kinds of resources, Fig. 11 shows the base case voltage profile and the improved voltage profile obtained when both populations react to the same signal. The maximum improvement in the voltage profile, when all resources are considered, is in the order of 6.5%.

In order to better understand how the different populations contribute to the control action, Fig. 12 shows the active power injected/absorbed by the SC array at bus 840 when they are the only controllable resources as well as when TCL and SC are coordinated. Also, in the same figure the aggregate active power of the elastic loads at the same bus is depicted for the same cases.

In Fig. 13 the median value SoC of the SC arrays is shown when only SC are controlled (solid line) and when both populations respond to the signals (dashed line). Overall, one can observe that when TCL are included in the control actions the response of the SC is smoothed. However, the amount of voltage profile improvement remains almost the same compared to the case of ESS only. This result is due to the fact that the designed control mechanism requires a given amount of power/energy per bus that can be provided by any resource connected to the considered bus.

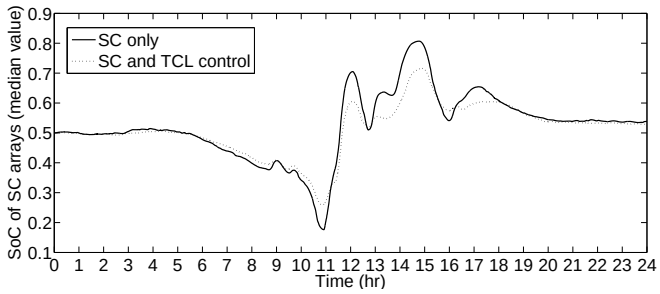

Figure 13. Median value of the 24hr SoC of the SC arrays when only SC are controlled and when SC and TCL are coordinated.

V. Conclusion

This paper has proposed the extension of a demand-response control mechanism based on low bit-rate broadcast signals, already presented by the authors in [17], to control both loads and distributed ESSs. The paper has verified the inherent flexibility of the proposed control scheme that is capable of controlling non-homogeneous populations of loads and ESSs to provide specific ancillary services to ADNs.

The paper has validated the proposed control mechanism by making reference to a typical IEEE 34 node distribution test feeder which was appropriately adapted in order to comprise distributed ESSs, a large population of heterogeneous household controllable loads along with non-elastic demand, as well as non-dispatchable power injections. The method is applied in detail to an ADN that uses Grid Explicit Congestion Notification (GECN) as broadcast signal and has been also used to size the ESSs. The results show that the proposed storage controller successfully contributes to primary voltage control in distribution networks. Specifically, the capability of controlling the voltage deviations via distributed storage can be up to 6% of the network's voltage rated value. Additionally, the results indicate that the same GECN control signals are able to sufficiently coordinate different energy resources as long as the latter are equipped with local controllers that can interpret the signal and respond according to their capabilities. The successful verification of the proposed control scheme makes it a good candidate for dedicated experimental deployment.

REFERENCES

[1] J. Lopes, N. Hatziargyriou, J. Mutale, P. Djapic, and N. Jenkins, "Integrating distributed generation into electric power systems: A review of drivers, challenges and opportunities," *Electric Power Systems Research*, vol. 77, no. 9, pp. 1189–1203, 2007.

[2] N. Singh, E. Kliokys, H. Feldmann, R. Kussel, R. Chrustowski, and C. Joborowicz, "Power system modelling and analysis in a mixed energy management and distribution management system," *IEEE Trans. Power Systems*, vol. 13, no. 3, pp. 1143–1149, 1998.

[3] N.-G. James, *Control and Automation of Electrical Power Systems*. Hoboken, NJ: CRC Press, 2006.

[4] T. Senjyu, Y. Miyazato, A. Yona, N. Urasaki, and T. Funabashi, "Optimal distribution voltage control and coordination with distributed generation," *IEEE Trans. Power Delivery*, vol. 23, no. 2, pp. 1236–1242, 2008.

[5] A. Borghetti, M. Bosetti, S. Grillo, S. Massucco, C. Nucci, M. Paolone, and F. Silvestro, "Short-term scheduling and control of active distribution systems with high penetration of renewable resources," *IEEE Systems Journal*, vol. 4, no. 3, pp. 313–322, 2010.

[6] Q. Zhou and J. Bialek, "Generation curtailment to manage voltage constraints in distribution networks," *IET Generation, Transmission & Distribution*, vol. 1, no. 3, pp. 492–498, 2007.

[7] "Capacity of distribution feeders for hosting der," *TB draft by WG C6.24 CIGRE*, 2013.

[8] European Network of Transmission System Operators for Electricity (ENTSO-E), "Draft network code on demand connection," December 5,2012.

[9] J. Wu, J. Ekanayake, and K. Samarakoon, "Frequency response from electric vehicles," in *ENERGY 2011, The First International Conference on Smart Grids, Green Communications and IT Energy-aware Technologies*, 2011, pp. 148–152.

[10] K. Samarakoon, J. Ekanayake, and N. Jenkins, "Investigation of Domestic Load Control to Provide Primary Frequency Response Using Smart Meters," *IEEE Trans. Smart Grid*, vol. 3, no. 1, pp. 282–292, 2012.

[11] M. Arnold and G. Andersson, "Model predictive control of energy storage including uncertain forecasts," in *Proc. PSCC*, 2011.

[12] S. Koch, F. Barcenas, and G. Andersson, "Using controllable thermal household appliances for wind forecast error reduction," in *IFAC Conference on Control Methodologies and Technology for Energy Efficiency*. Citeseer, 2010.

[13] H. E. Z. Farag and E. F. El-Saadany, "A novel cooperative protocol for distributed voltage control in active distribution systems," *IEEE Trans. Power Systems*, vol. PP, no. 99, pp. 1–1.

[14] H. Farag, E. El-Saadany, and R. Seethapathy, "A two ways communication-based distributed control for voltage regulation in smart distribution feeders," *IEEE Trans. Smart Grid*, vol. 3, no. 1, pp. 271–281, March.

[15] K. Turitsyn, N. Sinitsyn, S. Backhaus, and M. Chertkov, "Robust broadcast-communication control of electric vehicle charging," in *Smart Grid Communications (SmartGridComm), 2010 First IEEE International Conference on*, Oct., pp. 203–207.

[16] S. Bashash and H. Fathy, "Robust demand-side plug-in electric vehicle load control for renewable energy management," in *American Control Conference (ACC), 2011*, 29 2011-July 1, pp. 929–934.

[17] K. Christakou, D. Tomozei, J. Le Boudec, and M. Paolone, "GECN: Primary Voltage Control for Active Distribution Networks via Real-Time Demand-Response," *IEEE Trans. Smart Grid*, 2013, in press.

[18] Q. Zhou and J. Bialek, "Energy storage is a key smart grid element," in *Proc. of Cigré Symposium, The Electric Power System of the Future, Sept. 13-15, Bologna, Italy*, 2011.

[19] M. Nick, M. Hohmann, R. Cherkaoui, and M. Paolone, "On the optimal placement of distributed storage systems for voltage control in active distribution networks," in *Innovative Smart Grid Technologies (ISGT Europe), 2012 3rd IEEE PES International Conference and Exhibition*, Oct., pp. 1–6.

[20] L. Czarnecki and Z. Staroszczyk, "On-line measurement of equivalent parameters for harmonic frequencies of a power distribution system and load," *IEEE Trans. Instrumentation and Measurement,*, vol. 45, no. 2, pp. 467–472, 1996.

[21] K. Christakou, J. LeBoudec, M. Paolone, and D.-C. Tomozei, "Efficient computation of sensitivity coefficients of node voltages and line currents in unbalanced radial electrical distribution networks," *IEEE Trans. Smart Grid*, vol. 4, no. 2, pp. 741–750, 2013.

[22] S. Piller, M. Perrin, and A. Jossen, "Methods for state-of-charge determination and their applications," *Journal of power sources*, vol. 96, no. 1, pp. 113–120, 2001.

[23] B. Belvedere, M. Bianchi, A. Borghetti, C. Nucci, M. Paolone, and A. Peretto, "A microcontroller-based power management system for standalone microgrids with hybrid power supply," *IEEE Trans. Sustainable Energy*, vol. 3, no. 3, pp. 422–431, July.

[24] V. Pop, H. J. Bergveld, P. Notten, and P. P. Regtien, "State-of-the-art of battery state-of-charge determination," *Measurement Science and Technology*, vol. 16, no. 12, p. R93, 2005.

[25] I. Papic, "Simulation model for discharging a lead-acid battery energy storage system for load leveling," *IEEE Trans. Energy Conversion*, vol. 21, no. 2, pp. 608–615, 2006.

[26] M. Coleman, C. K. Lee, C. Zhu, and W. G. Hurley, "State-of-charge determination from emf voltage estimation: Using impedance, terminal voltage, and current for lead-acid and lithium-ion batteries," *IEEE Trans. Industrial Electronics*, vol. 54, no. 5, pp. 2550–2557, 2007.

[27] B. Yann Liaw, G. Nagasubramanian, R. G. Jungst, and D. H. Doughty, "Modeling of lithium ion cells a simple equivalent-circuit model approach," *Solid state ionics*, vol. 175, no. 1, pp. 835–839, 2004.

[28] S. R. Nelatury and P. Singh, "Equivalent circuit parameters of nickel/metal hydride batteries from sparse impedance measurements," *Journal of power sources*, vol. 132, no. 1, pp. 309–314, 2004.

[29] A. J. Salkind, P. Singh, A. Cannone, T. Atwater, X. Wang, and D. Reisner, "Impedance modeling of intermediate size lead–acid batteries," *Journal of power sources*, vol. 116, no. 1, pp. 174–184, 2003.

[30] T. B. Reddy, *Linden's Handbook of Batteries*. McGraw-Hill, 2011, vol. 4.

[31] R. G. Valle and J. A. P. Lopes, *Electric vehicle integration into modern power networks*. Springer, 2012, vol. 2.

[32] L. Zubieta and R. Bonert, "Characterization of double-layer capacitors for power electronics applications," *IEEE Trans. Industry Applications*, vol. 36, no. 1, pp. 199–205, 2000.

[33] D. Torregrossa, M. Bahramipanah, E. Namor, R. Cherkaoui, and M. Paolone, "Improvement of dynamic modeling of supercapacitor by residual charge effects estimation," *IEEE Trans. Industrial Electronics*, vol. PP, no. 99, pp. 1–1, 2013.

[34] Q. Zhou and J. Bialek, "Simplified calculation of voltage and loss sensitivity factors in distribution networks," in *Proc. of the 16th Power Systems Computation Conference (PSCC2008), Glasgow, Scotland*, 2008.

[35] W. Kersting, "Radial distribution test feeders," in *Power Engineering Society Winter Meeting, 2001. IEEE*, vol. 2, 2001, pp. 908–912 vol.2.

[36] M. Eremia and M. Shahidehpour, *Handbook of Electrical Power System Dynamics: Modeling, Stability, and Control*. Wiley-IEEE Press, 2013, vol. 92.